Iranian Journal of Basic Medical Sciences
ijbms.mums.ac.ir

HIPK2 protects neurons from oxidative stress and modulates central nervous system responses following traumatic brain injury

Qiangbin Zhu [1], Fan Wang [1], Bojun Zhang [1], Zhigang Pan [1], Xiaodong Kang [2], Weipeng Hu [1]*

[1] Department of Neurosurgery, The Second Affiliated Hospital of Fujian Medical, Quanzhou, Fujian Province, China
[2] Department of Intensive Care Unit, The Second Affiliated Hospital of Fujian Medical, Quanzhou, Fujian Province, China

ARTICLE INFO

Article type:
Original

Article history:
Received: Aug 17, 2025
Accepted: Mar 8, 2026

Keywords:
Anti-oxidant response
HIPK2
Neuroprotection
Oxidative stress
Traumatic brain injury

ABSTRACT

Objective(s): Traumatic brain injury (TBI) induces oxidative stress, contributing to secondary neuronal damage. This study aimed to elucidate the role of the stress-responsive kinase HIPK2 in regulating endogenous antioxidant defenses in neural tissue following TBI.

Materials and Methods: We employed complementary *in vitro* and *in vivo* models: an H_2O_2-induced oxidative stress model in PC12 cells (with HIPK2 inhibited by siRNA) and a controlled cortical impact mouse model of TBI (with HIPK2 overexpressed via intracerebroventricular Ad-HIPK2 injection). Analyses included assessments of cell viability, mRNA expression, and protein levels of key antioxidant factors (HO-1, UGT1A1, NQO1).

Results: *In vitro*, HIPK2 inhibition markedly increased oxidative stress-induced cell death and significantly down-regulated UGT1A1 expression. *In vivo*, endogenous HIPK2 expression was significantly suppressed post-TBI. Conversely, HIPK2 overexpression effectively rescued the expression of antioxidant proteins UGT1A1 and NQO1.

Conclusion: These results demonstrate that HIPK2 is a critical modulator of the antioxidant response after TBI, capable of orchestrating key defense genes and conferring neuroprotection. Our findings identify HIPK2 as a promising molecular target for therapeutic intervention against TBI-related oxidative damage.

▶Please cite this article as:
Zhu Q, Wang F, Zhang B, Pan Zh, Kang X, Hu W. HIPK2 protects neurons from oxidative stress and modulates central nervous system responses following traumatic brain injury. Iran J Basic Med Sci 2026; 29:

Introduction

Traumatic brain injury (TBI) is the third most common neurological disorder, yet its pathophysiological mechanisms remain complex and incompletely understood (1). Among traumatic injuries, severe TBI carries a mortality rate of 30%–40% (2), and most survivors experience lasting neurological impairments (3), contributing to an estimated global economic burden of approximately $400 billion annually (4). Despite the availability of multiple treatment strategies, no markedly effective therapeutic interventions have been established (1). Therefore, elucidating the pathophysiological mechanisms of TBI and identifying more effective therapeutic targets are essential for improving acute TBI survival rates and reducing the associated societal and economic burden.

Oxidative stress refers to a relative excess of reactive oxygen species (ROS) resulting from either increased ROS production or impaired ROS clearance (5), ROS are highly reactive oxygen-containing molecules, including oxygen-derived free radicals and reactive non-radical species such as O_2^-, hydrogen peroxide (H_2O_2), NO, and $ONOO^-$ (6). In mammalian cells, endogenous ROS are primarily generated in organelles such as mitochondria and the endoplasmic reticulum (7). The balance between oxidative stress and antioxidant defenses is essential for regulating the neuroinflammatory response following TBI (8). Uridine diphosphate glucuronosyltransferase 1A1 (UGT1A1) can be up-regulated by transcription factors such as nuclear factor erythroid 2–related factor 2 (Nrf2) (9). Nrf2 plays a key role in detoxification and redox homeostasis, contributing to the physiological expression of multiple genes regulated by antioxidant response elements (10). After TBI, cellular ischemia, hypoxia, mitochondrial swelling, and elevated ROS production, combined with excessive consumption of ROS scavengers, lead to the inactivation of antioxidant systems. This disruption of the balance between ROS generation and elimination results in ROS accumulation and subsequent brain tissue damage, ultimately contributing to neurological impairment (11, 12). In response, the body activates antioxidative mechanisms, inducing key antioxidant factors such as heme oxygenase-1 (HO-1), UGT1A1, and NAD(P)H quinone oxidoreductase 1 (NQO1) (13, 14, 9).

***Corresponding author:** Weipeng Hu. Department of Neurosurgery, The Second Affiliated Hospital of Fujian Medical University, Donghai Street No.950, Quanzhou 362000, China. Tel: +86 0595-26655286, Fax: +86 0595-26655286, Email: hwpfjmu@yeah.net

Homeodomain-interacting protein kinase 2 (HIPK2), a member of the serine/threonine kinase family, is localized in the cell nucleus and plays an essential role in cell-cycle regulation. HIPK2 exerts its biological functions through multiple post-translational modifications, including ubiquitination, SUMOylation, acetylation, and phosphorylation, which together regulate transcription, as well as cell differentiation, proliferation, and apoptosis (15-19). HIPK2 is also involved in cellular oxidative stress responses and promotes cell survival under conditions of elevated ROS (20). Previous studies have shown that HIPK2 overexpression in a rat spinal cord injury model improves the inflammatory response, enhances functional recovery, and reduces edema (21). However, the expression pattern of HIPK2 in TBI and its role in oxidative stress regulation within the nervous system remain poorly defined.

Highly differentiated PC12 cells serve as an important model for studying neuronal function and disease mechanisms. Upon NGF induction, PC12 cells acquire neuronal properties, making them widely used in neuroscience research (22). In this study, we established an oxidative stress model in PC12 cells to investigate the role of HIPK2 in neuronal oxidative stress. In parallel, we developed a mouse TBI model to examine HIPK2 expression in the central nervous system following injury and to evaluate its influence on the oxidative stress response.

Materials and Methods

Cell culture and treatment

The highly differentiated PC12 cells used in this study were purchased from Shanghai Anwei Biotechnology Co., Ltd. PC12 cells are widely utilized in neurological research because of their strong differentiation capacity, which enables them to model neuronal responses to injury (22). In this experiment, the cells were cultured in complete medium consisting of RPMI-1640 (BasalMedia, China), 10% fetal bovine serum (FBS; Gibco, USA), and 1% penicillin–streptomycin (P/S; Beyotime, China) in a humidified incubator containing 95% air and 5% CO_2 at 37 °C. Subculturing was performed twice per week. Cells used in this study were between passages 4 and 5 and were fully differentiated.

For cryopreservation, cells were first cooled at 4 °C for 30 min, then transferred to −20 °C for 2 hr, followed by overnight storage at −80 °C before long-term storage in liquid nitrogen. For adherent cultures, cells were dissociated using 0.25% trypsin (Beyotime, China) (suspension cells were collected directly), and the resulting cell suspension was cryopreserved using the same procedure. After centrifugation at 1000 rpm for 5 min, the supernatant was removed and the cell pellet was resuspended in cryopreservation medium at a final concentration of approximately 10^6 cells/ml. Aliquots of 1 ml were dispensed into cryovials. The cryopreservation medium consisted of 55% basal medium, 40% FBS, and 5% dimethyl sulfoxide (DMSO; Sigma, USA).

Cell viability

Cells were allocated into groups according to the experimental design, and the cell concentration was adjusted to 5×10^4 cells/ml. A total of 100 µl of the cell suspension was seeded into each well of a 96-well plate, with six replicates per group. The plates were then placed in an incubator at 37 °C with 5% CO_2 and cultured for 24 hr. After the required pretreatments were applied, 10 µl of CCK-8 solution (Beyotime, China) was added to each well, followed by incubation for 1.5 hr. Absorbance at 450 nm was then measured using a microplate reader.

Three groups were included in the assay:
- Blank group: culture medium without cells or CCK-8.
- Control group: untreated cells with culture medium and CCK-8.
- Experimental group: treated cells with toxicant-containing medium and CCK-8.

Cell viability was calculated using the following formula:

$$\text{Cell viability (\%)} = [(A_{exp} - A\_b_{lank}) / (A\_c_{ontrol} - A\_b_{lank})] \times 100\%.$$

qPCR

Total RNA was extracted using RNAiso Plus reagent (Takara, Cat. No. 9109) according to the manufacturer's instructions. RNA concentration and purity were determined at 260 nm using a microvolume spectrophotometer. First-strand cDNA was synthesized from the isolated RNA using the PrimeScript™ RT reagent kit, following Sean Taylor's optimized reverse transcription protocol to ensure high efficiency (23). The resulting cDNA served as the template for subsequent quantitative real-time PCR (qPCR) analysis.

qPCR was performed using PerfectStart® Green qPCR SuperMix (Quanzhijin, Cat. No. AQ601-02) on a qTOWER 3G fluorescence-based real-time PCR system (Analytik Jena AG). The amplification program consisted of an initial denaturation at 94 °C for 30 sec, followed by 40 cycles of denaturation at 94 °C for 5 sec and annealing/extension at 60 °C for 30 sec. Relative gene expression levels were quantified using the comparative Ct method. For each sample, the Ct value was defined as the arithmetic mean of three technical replicates. Gene expression was normalized to the endogenous control GAPDH using the ΔCt method [ΔCt = Ct(target gene) − Ct(GAPDH)]. The relative fold change was calculated using the ΔΔCt method [ΔΔCt = ΔCt(experimental group) − mean ΔCt(control group)] and expressed as 2^(−ΔΔCt). Primer sequences are listed in Table 1.

Establishment of the TBI model

All mice were housed under standard laboratory conditions in a specific pathogen-free (SPF) facility with a controlled environment (temperature: 22 ± 2 °C; humidity: 50 ± 10%; 12-hour light/dark cycle). Animals had ad libitum access to autoclaved food and water. All animal procedures were approved by the Animal Ethics Committee of the Second Affiliated Hospital of Fujian Medical University (Approval No. 2021533) and conducted in accordance with the National Institutes of Health (NIH) Guide for the Care and Use of Laboratory Animals.

For TBI induction, mice were anesthetized with isoflurane (3–5% for induction and 1–2% for maintenance) and placed in a prone position on a stereotaxic cranial injury apparatus. The scalp was disinfected with alcohol-soaked cotton, and a midline incision was made to expose the right parietal bone following periosteal detachment. A 5-mm craniotomy was performed using a bone drill at coordinates 1.5 mm posterior and 2.5 mm lateral to the coronal suture, while ensuring the dura mater remained intact. An impact rod was positioned onto the dura, and a steel ball was released from

Table 1. Sequences of primers used for qPCR analysis in this study

Primer name	Sequence
HIPK2-F	5'-CATGACGCACCTACTGGATTTT-3'
HIPK2-R	5'-CGGGATTGGCTAAGGAAAGAG-3'
HO-1-F	5'-AGCGAAACAAGCAGAACCCA-3'
HO-1-R	5'-CCACCAGCAGCTCAGGATG-3'
NQO1-F	5'-GCGTCTGGAGACTGTCTGGG-3'
NQO1-R	5'-ATCTGGTTGTCGGCTGGAAT-3'
UGT1A1-F	5'-GCTCGGAGTTATTCAGCAGC-3'
UGT1A1-R	5'-TCCACAAAAGCAGCTGTCAC-3'
GAPDH-F	5'-GGCACAGTCAAGGCTGAGAATG-3'
GAPDH-R	5'-ATGGTGGTGAAGACGCCAGTA-3'

a height of 30 cm to strike the rod, producing a controlled cortical impact. The scalp incision was then sutured. Sham-operated mice received craniotomy only, with all other procedures identical to those of the TBI group. After regaining consciousness and stabilization of vital signs, mice were labeled according to group assignment and returned to their cages for postoperative observation (24).

Humane endpoints

To minimize animal suffering, predefined humane endpoints were strictly observed. Animals were immediately euthanized if they exhibited:

- Severe clinical distress, such as prolonged lethargy, inability to eat or drink, labored breathing, or neurological deficits (e.g., seizures or paralysis).
- Weight loss ≥20% of baseline body weight within 48–72 hr.

Euthanasia and death verification

Euthanasia was performed using gradual-fill CO_2 inhalation (displacement rate: 20–30% of chamber volume per minute), followed by a secondary physical method—cervical dislocation or bilateral thoracotomy—to ensure death. Death was confirmed by:

- Absence of heartbeat for 1 min
- Pupillary dilation with loss of corneal reflex
- Cyanosis of mucous membranes.

Animals and grouping

A total of 24 male C57BL/6J mice (6–8 weeks old, 18–22 g) were obtained from Beijing SPF Biotechnology Co., Ltd. (License No. SCXK (Beijing) 2019-0010). Fifteen mice were randomly assigned to the Sham and TBI groups, with the TBI group further subdivided into four time-point subgroups (1, 3, 7, and 14 days post-injury), resulting in five experimental groups (n = 3 per group). Brain tissues were collected at the designated time points following euthanasia.

The remaining nine mice were randomly allocated to the Sham, TBI, and TBI + Ad-HIPK2 groups (n = 3 per group). Mice in the TBI + Ad-HIPK2 group received a single intracerebroventricular (ICV) injection of Ad-HIPK2 adenovirus (5×10^9 PFU/ml, 1 µl; Shanghai Genechem Co., Ltd.) three days prior to TBI induction. Prior to injection, mice were anesthetized with isoflurane (3–5% for induction and 1–2% for maintenance). The scalp was disinfected with 75% ethanol, and a midline incision was made to expose the skull. A burr hole was drilled 2 mm posterior to the bregma and 1.5 mm lateral to the sagittal suture to target the right lateral ventricle. Bone debris was removed by rinsing with sterile 0.9% sodium chloride solution. A microinjection syringe mounted on a stereotaxic apparatus was then inserted 2 mm below the skull surface, and the viral suspension was slowly infused (1 µl over 1 minute). The needle was kept in place for an additional minute to prevent reflux before withdrawal. The incision was closed with absorbable sutures or surgical clips, and postoperative monitoring was performed to assess potential complications.

TBI was induced three days after viral administration using the previously described procedure. Sham controls underwent craniotomy without impact. Mice were euthanized, and tissues were harvested three days after TBI.

Tissue collection

Mice were euthanized by isoflurane overdose (5% in oxygen for 3–5 min in an induction chamber). Following confirmation of the absence of respiration and heartbeat, animals were decapitated, and the brains were rapidly removed on ice. Tissues were then stored at −80 °C for subsequent western blot analysis.

Western blot

Brain tissues were homogenized in RIPA buffer (Meilunbio, MA0151) supplemented with protease and phosphatase inhibitors (Meilunbio MB2678, MB12707, PMSF) using a TISS-24 tissue grinder. Homogenates were incubated on ice for 30 min and centrifuged at 12,000 × g for 20 min at 4 °C. Supernatants were collected for protein quantification. Protein concentrations were determined using a BCA kit (Meilunbio, MA0082-2). Lysates were diluted, mixed with working reagent, incubated at 60 °C for 20 min, and measured at 570 nm. All samples were adjusted to 2 µg/µl with RIPA buffer. For western blotting, 20 µg of protein per sample was denatured, separated on 10% SDS-PAGE gels, and transferred to PVDF membranes (PALL, BSP0160). Membranes were blocked with 5% skim milk and incubated overnight at 4 °C with primary antibodies against GAPDH (1:40,000), HIPK2 (1:10,000), HO-1, NQO1, and UGT1A1 (1:8,000–1:10,000). HRP-conjugated secondary antibodies (1:10,000) were applied for 1 hour at room temperature. Protein bands were visualized using ECL reagent and quantified with ImageJ. Intensities were background-subtracted and normalized to GAPDH. All experiments were performed in triplicate.

Statistical analysis

Statistical analyses were performed using SPSS version 23.0 (IBM Corp., Armonk, NY, USA). Continuous variables are presented as mean ± standard deviation (SD). Data normality was assessed using the Shapiro–Wilk test (P>0.05 indicating normal distribution), and homogeneity of variance was evaluated with Levene's test (P>0.05 indicating equal variances). Between-group differences were analyzed using unpaired Student's t-tests for normally distributed data or the Mann–Whitney U test for non-normal distributions. For comparisons among multiple groups, one-way ANOVA

was conducted. Tukey's *post hoc* test was applied for qPCR data when parametric assumptions were met, whereas Fisher's least significant difference (LSD) test was used for western blot quantification. When parametric assumptions were violated, the Kruskal–Wallis test followed by Dunn's *post hoc* correction was used. A two-tailed *P*-value<0.05 was considered statistically significant.

Results

PC12 cells were exposed to various concentrations of H_2O_2 (0, 50, 100, 300, and 500 μM) for 24 hr to induce oxidative stress. Cell viability decreased in a concentration-dependent manner, with all treatment groups showing statistically significant reductions compared with the control (P<0.05) (Figure 1). These results indicate that H_2O_2-induced oxidative stress leads to cell death, with higher concentrations producing more pronounced cytotoxic effects. tBID, a selective inhibitor of HIPK2 with an IC_{50} of 0.33 μM, was used to examine the role of HIPK2 in oxidative stress. Accordingly, cells were assigned to three groups: control, H_2O_2-treated, and tBID + H_2O_2.

Based on preliminary experiments, 100 μM H_2O_2 was selected to establish an oxidative stress model in PC12 cells. Cells in the H_2O_2 group were treated with 100 μM H_2O_2 for 24 hr, whereas those in the tBID + H_2O_2 group were pretreated with 1/4 IC_{50} tBID for 6 hr followed by co-incubation with 100 μM H_2O_2. Control cells received an equivalent volume of saline. Gene expression was quantified by qPCR, and cell viability was assessed using the CCK-8 assay.

As shown in Table 2, H_2O_2 exposure significantly increased the mRNA expression of HO-1, UGT1A1, and NQO1 compared with the control group (P<0.05), confirming a robust oxidative stress response. Following HIPK2 inhibition by tBID, the tBID + H_2O_2 group exhibited

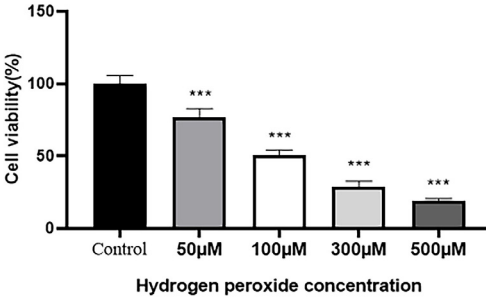

Figure 1. Hydrogen peroxide (H_2O_2) decreases cell viability in a dose-dependent manner in PC12 cells
Cell viability was measured after treatment with increasing concentrations (50–500 μM) of hydrogen peroxide (H_2O_2). Data are presented as mean ± standard deviation (SD) (n = 8). Statistical significance was evaluated relative to the control group, with significance defined as P<0.05. ***P<0.001.

significantly reduced HIPK2 and UGT1A1 mRNA levels relative to the H_2O_2 group (P<0.05). Although HO-1 and NQO1 expression showed a downward trend, these changes were not statistically significant (P>0.05; Figure 2a-d). Moreover, HIPK2 inhibition significantly increased cell death (P<0.05; Figure 2e). Collectively, these results suggest that HIPK2 regulates cellular oxidative stress responses by modulating UGT1A1 expression and plays a protective role against neuronal oxidative stress.

Data from the PC12 cell oxidative stress model, including cell viability (CCK-8) and gene expression (qPCR), are provided in Supplementary File 1. Oxidative stress is a major contributor to secondary neuronal injury following TBI (8). To further investigate the role of HIPK2 in TBI, a mouse TBI model was established to evaluate HIPK2 expression in brain tissue at 1, 3, 7, and 14 days post-injury. Western blot analysis was performed to quantify HIPK2 protein levels. Notably, contrary to expectations based on *in vitro* findings,

Table 2. Effects of H_2O_2 and HIPK2 inhibition on mRNA expression of target genes

	Group	Mean ΔCt ± SD	F (*P*-value)	ANOVA (*P*-value)	Comparison	*P*-value (Tukey's HSD)
HIPK2	Control	8.838 ± 0.175	5.091 (0.051)	0.030*	vs H_2O_2	0.058
					vs tBID+H_2O_2	0.924
	H_2O_2	7.747 ± 0.287			vs tBID+H_2O_2	0.037*
	tBID+H_2O_2	8.979 ± 0.711			vs H_2O_2	0.037
HO-1	Control	4.358 ± 0.186	0.733 (0.519)	0.000***	vs H_2O_2	0.000***
					vs tBID+H_2O_2	0.001**
	H_2O_2	2.430 ± 0.305			vs tBID+H_2O_2	0.053
	tBID+H_2O_2	3.034 ± 0.228			vs H_2O_2	0.053
NQO1	Control	0.243 ± 0.205	3.235 (0.111)	0.004*	vs H_2O_2	0.005**
					vs tBID+H_2O_2	0.009**
	H_2O_2	-0.960 ± 0.127			vs tBID+H_2O_2	0.794
	tBID+H_2O_2	-0.808 ± 0.426			vs H_2O_2	0.794
UGT1A1	Control	11.672 ± 0.063	2.291 (0.182)	0.025*	vs H_2O_2	0.032*
					vs tBID+H_2O_2	0.967
	H_2O_2	10.382 ± 0.459			vs tBID+H_2O_2	0.044*
	tBID+H_2O_2	11.579 ± 0.651			vs H_2O_2	0.044*

Data are presented as mean ΔCt ± SD (n=3). *P<0.05, **P<0.01, ***P<0.001. ΔCt: delta cycle threshold; SD: standard deviation; ANOVA: analysis of variance; HSD: honestly significant difference; H_2O_2: hydrogen peroxide

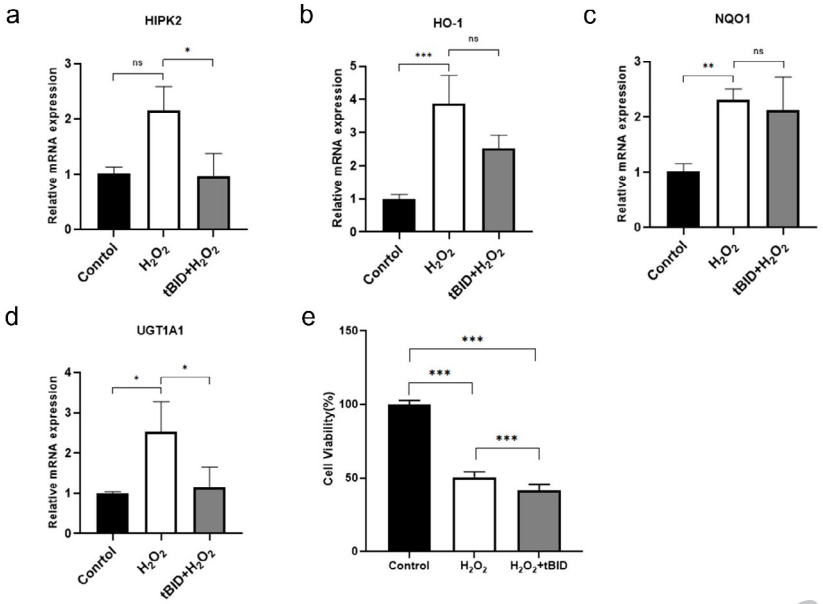

Figure 2. (a–d) Effects of different treatments on the mRNA expression of HIPK2, HO-1, NQO1, and UGT1A1. The mRNA expression levels of (a) HIPK2, (b) HO-1, (c) NQO1, and (d) UGT1A1 were measured in control, hydrogen peroxide (H_2O_2)-treated, and tBID + H_2O_2-treated groups of PC12 cells by qPCR. Data are from three independent experiments with triplicate technical repeats per experiment, normalized to the control group, and presented as mean ± standard deviation (SD). Statistical analysis was performed using one-way ANOVA followed by Tukey's *post hoc* test. (e) Effects of different treatments on cell viability. Cell viability was measured using the CCK-8 assay. Statistical analysis was performed using one-way ANOVA followed by LSD *post hoc* test. Significance is denoted at $P<0.05$.
HIPK2: Homeodomain-interacting protein kinase 2; HO-1: heme oxygenase-1; NQO1: NAD(P)H Quinone Dehydrogenase 1; UGT1A1: UDP-glucuronosyltransferase 1A1; tBID: truncated BID; qPCR: quantitative real-time polymerase chain reaction; ANOVA: analysis of variance; CCK-8: Cell Counting Kit-8; LSD: least significant difference

HIPK2 expression was reduced rather than elevated following TBI. Representative western blot images (Figure 3a) and corresponding densitometric analysis (Figure 3b) showed that HIPK2 protein levels were significantly decreased at all post-injury time points compared with the sham group ($P<0.05$). HIPK2 expression declined sharply on day 1 and gradually recovered beginning on day 3, although levels remained significantly lower than those in sham controls. All gel images were uniformly adjusted for brightness and contrast. These findings indicate that TBI dynamically regulates HIPK2 expression in neural tissue.

Previous *in vitro* experiments indicated that HIPK2 participates in the regulation of cellular oxidative stress. To determine whether HIPK2 similarly modulates oxidative stress following TBI, the 3-day post-injury time point was selected. Mice were assigned to three groups: sham, TBI, and TBI + Ad-HIPK2. The TBI + Ad-HIPK2 group received an intracerebroventricular injection of recombinant HIPK2 (Shanghai Genechem Co., Ltd.) to induce HIPK2 overexpression. Western blotting was performed to assess oxidative stress-related proteins, including HO-1, UGT1A1, and NQO1, in brain tissue.

Representative western blot images (Figure 4a) and corresponding densitometric analysis (Figure 4b) demonstrated that HIPK2 overexpression significantly increased UGT1A1 and NQO1 expression compared with the TBI group ($P<0.05$). Although HO-1 expression exhibited a slight upward trend, the increase was not statistically significant ($P>0.05$). All gel images were uniformly adjusted for brightness and contrast. Collectively, these results suggest that HIPK2 contributes to the oxidative stress response in neural tissue following TBI and may serve a neuroprotective role.

Data from the *in vivo* TBI mouse model, including the temporal profile of HIPK2 protein expression and the subsequent alterations in oxidative stress-related proteins (HO-1, UGT1A1, NQO1) following HIPK2 overexpression as assessed by western blot, are provided in Supplementary File 2.

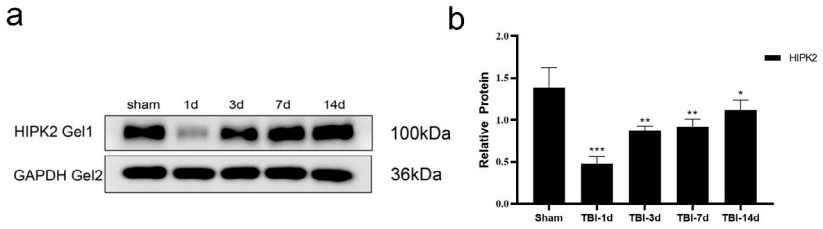

Figure 3. Temporal changes in HIPK2 protein expression following mouse TBI
(a) Representative western blot bands of HIPK2 in the cerebral cortex of sham-operated rats and at indicated time points post-TBI. GAPDH served as the loading control. (b) Quantitative analysis of HIPK2 protein expression. Data are presented as mean ± standard deviation (SD) (n = 3). Statistical analysis was performed using one-way analysis of variance (ANOVA) followed by LSD *post hoc* test.
HIPK2: Homeodomain-Interacting Protein Kinase 2; TBI: Traumatic brain injury; LSD: least significant difference; GAPDH: Glyceraldehyde-3-phosphate dehydrogenase

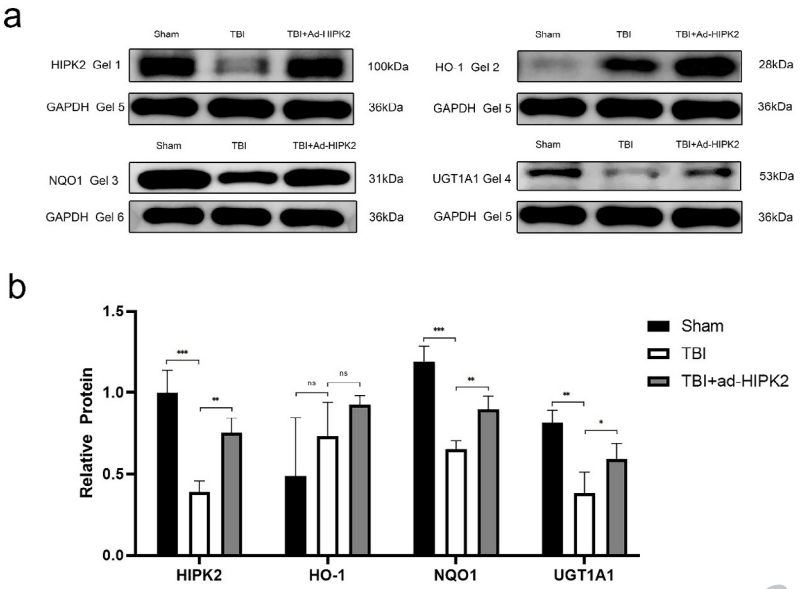

Figure 4. Effects of HIPK2 overexpression on anti-oxidant pathway proteins following TBI in mice
(a) Representative western blot bands showing the expression levels of HIPK2, HO-1, NQO1, and UGT1A1 in each group, with GAPDH used as the internal reference protein. Mice in the TBI + adenovirus-mediated HIPK2 overexpression (Ad-HIPK2) group received intracerebroventricular injection of recombinant adenovirus encoding HIPK2. (b) Bar graph of quantitative statistical analysis. Statistical analysis was performed using one-way ANOVA followed by LSD *post hoc* test.
HIPK2: Homeodomain-Interacting Protein Kinase 2; TBI: Traumatic brain injury; LSD: least significant difference; GAPDH: Glyceraldehyde-3-phosphate dehydrogenase; HO-1: Heme Oxygenase-1; NQO1: NAD(P)H Quinone Dehydrogenase 1; UGT1A1: UDP-glucuronosyltransferase 1A1 ; ANOVA: analysis of variance

Discussion

Secondary neuronal injury following TBI is a complex pathophysiological process involving microglial activation, inflammation, Ca^{2+} overload, oxidative stress, and mitochondrial dysfunction (8, 12, 25-27), Among these factors, oxidative stress plays a central role in secondary neuronal damage. It is activated during the acute phase of TBI and can exacerbate primary injury, ultimately contributing to neurological dysfunction (28).

The antioxidant defense system mitigates excessive ROS and is divided into enzymatic and non-enzymatic components. Enzymatic antioxidants include superoxide dismutase, glutathione peroxidase, and catalase, whereas non-enzymatic antioxidants include glutathione and NADPH (29,30). NQO1 is a widely distributed FAD-dependent flavoprotein that catalyzes the reduction of quinones, quinone imines, nitroaromatic compounds, and azo dyes (31). NQO1 responds to oxidative stress and exhibits direct antioxidant activity, including partial scavenging of superoxide radicals (13, 32-34), In Alzheimer's disease, increased NQO1 expression is considered a protective response to neuronal oxidative stress (35). HO-1is highly sensitive to pro-oxidative stimuli (36) and functions as a cytoprotective protein (37). HO-1 helps maintain mitochondrial integrity and promotes cell survival by reducing oxidative stress and inflammation (14).

HIPK2 is a stress-responsive kinase expressed at significantly higher levels in the central nervous system than in other tissues (38). Under basal, non-oxidative stress conditions, HIPK2 undergoes SUMOylation and binds to HDAC3, maintaining a deacetylated state (39). Excessive ROS levels inhibit HIPK2 SUMOylation, reducing its interaction with HDAC3 and leading to HIPK2 acetylation (15). Acetylated HIPK2 has been reported to protect cells and promote survival under conditions of elevated oxidative stress (16).

In our *in vitro* experiments, oxidative stress markedly increased HIPK2 mRNA expression, and inhibition of HIPK2 reduced cell viability, indicating that HIPK2 may contribute to the regulation of cell survival under stress conditions. This interpretation is supported by previous findings showing elevated HIPK2 expression in neurons within the perilesional cortex of a rat TBI model (40). In contrast, our mouse model of TBI exhibited an overall reduction in HIPK2 protein levels in whole-brain tissue after injury.

This discrepancy may arise from differences in experimental approaches and the spatial resolution of the analyses. Earlier studies concentrated on the perilesional cortex, a penumbral region adjacent to the injury core where severe stress rapidly induces localized HIPK2 activation and accumulation during the acute phase. By comparison, our measurements were based on whole-brain homogenates, which include not only this region but also the injury core—characterized by extensive cellular destruction—as well as the contralateral hemisphere and distant areas that experience minimal impact. As a result, the strong local up-regulation of HIPK2 is diluted and offset by the predominantly low expression in unaffected tissue and by protein degradation in necrotic regions, leading to an overall decrease at the whole-brain level. Additionally, HIPK2 has been reported to undergo ubiquitin-mediated degradation under stress conditions such as hypoxia (41), further supporting a mechanistic explanation for the reduced protein levels observed here. Collectively, these findings suggest that the divergent patterns of HIPK2 expression at regional versus whole-brain scales after TBI reflect the complex spatiotemporal dynamics of its regulation following injury. *In vitro* experiments demonstrated that HIPK2 inhibition significantly down-regulated UGT1A1 levels. A concurrent downward trend in HO-1 expression was observed, though not statistically significant (P=0.53), suggesting the need for verification through studies with larger sample sizes. Furthermore, HIPK2 conferred protective effects against

H_2O_2-induced oxidative damage in PC12 cells.

Although HIPK2 regulation of NQO1 expression could not be definitively demonstrated *in vitro*, HIPK2 overexpression *in vivo* significantly increased NQO1 levels. While HO-1 expression did not reach statistical significance *in vivo*, a trend toward elevation was observed (P>0.05). Collectively, these findings suggest that HIPK2 may contribute to the neuronal oxidative stress response following TBI and enhance cellular resilience against oxidative damage.

Limitations

This study has several limitations. First, in the *in vitro* experiments, only the baseline mRNA expression levels of HIPK2, HO-1, UGT1A1, and NQO1 were measured, without assessment of the corresponding protein levels. This limitation should be addressed in future studies. Second, the mechanisms by which HIPK2 regulates HO-1, UGT1A1, and NQO1 were not explored. Future research should focus on elucidating the specific pathways through which HIPK2 modulates neuronal tolerance to oxidative stress following TBI.

Conclusion

HIPK2 regulates UGT1A1 expression in PC12 cells under oxidative stress, thereby modulating cellular oxidative stress responses. Additionally, HIPK2 protects PC12 cells against H_2O_2-induced oxidative damage. In a murine TBI model, HIPK2 expression is markedly down-regulated in brain tissue. Notably, HIPK2 overexpression increases UGT1A1 and NQO1 expression, highlighting its critical role in regulating the neuronal oxidative stress response following TBI. These findings identify HIPK2 as a potential therapeutic target for TBI.

Acknowledgment

This work was supported by Natural Science Foundation of Fujian Province, China [grant NO.2022J01781].

Authors' Contributions

Q Z, F W, B Z, Z P, X K, and W H contributed to study conception and design; Q Z and F W performed investigation, data collection, and drafted the manuscript; B Z, Z P, and X K contributed to methodology and data curation; W H supervised the study, acquired funding, and revised the manuscript.

Data Availability Statement

The datasets generated and/or analyzed during the current study, including the original uncropped blots and replicates, are available from the corresponding author upon reasonable request.

Ethical Approval Statement

This study was approved by the Ethics Committee of Experimental Animals at the Second Affiliated Hospital of Fujian Medical University, China (Ethical Number: 2021533).

Conflicts of Interest

The authors declare that they have no known competing financial interests or personal relationships that could influence the work reported in this paper.

Declaration

We have not used any AI tools or technologies to prepare this manuscript.

References

1. Kabadi S, Faden A. Neuroprotective strategies for traumatic brain injury: improving clinical translation. Int J Mol Sci 2014;15:1216-1236.
2. Rosenfeld JV, Maas AI, Bragge P, Morganti-Kossmann MC, Manley GT, Gruen RL. Early management of severe traumatic brain injury. Lancet 2012;380:1088-1098.
3. Hazeldine J, Lord JM, Belli A. Traumatic brain injury and peripheral immune suppression: Primer and prospectus. Front Neurol 2015;6:235.
4. Maas AIR, Menon DK, Adelson PD, Andelic N, Bell MJ, Belli A, *et al.* Traumatic brain injury: Integrated approaches to improve prevention, clinical care, and research. Lancet Neurol 2017;16:987-1048.
5. Chiang S, Chen S, Chang L. The role of ho-1 and its crosstalk with oxidative stress in cancer cell survival. Cells 2021;10:2401.
6. Zhang R, Xu M, Wang Y, Xie F, Zhang G, Qin X. Nrf2—a promising therapeutic target for defensing against oxidative stress in stroke. Mol Neurobiol 2017;54:6006-6017.
7. Radermacher KA, Wingler K, Langhauser F, Altenhofer S, Kleikers P, Hermans JJ, *et al.* Neuroprotection after stroke by targeting nox4 as a source of oxidative stress. Antioxid Redox Signal 2013;18:1418-1427.
8. Chen X, Wang H, Zhou M, Li X, Fang Z, Gao H, *et al.* Valproic acid attenuates traumatic brain injury-induced inflammation in vivo: involvement of autophagy and the nrf2/are signaling pathway. Front Mol Neurosci 2018;11:117.
9. Buckley DB, Klaassen CD. Induction of mouse udp-glucuronosyltransferase mrna expression in liver and intestine by activators of aryl-hydrocarbon receptor, constitutive androstane receptor, pregnane x receptor, peroxisome proliferator-activated receptor α, and nuclear factor erythroid 2-related factor 2. Drug Metab Dispos 2009;37:847-856.
10. Wang Y, Sun W, Du B, Miao X, Bai Y, Xin Y, *et al.* Therapeutic effect of mg-132 on diabetic cardiomyopathy is associated with its suppression of proteasomal activities: roles of nrf2 and nf-κb. Am J Physiol-Heart C 2013;304:H567-H578.
11. Roth TL, Nayak D, Atanasijevic T, Koretsky AP, Latour LL, McGavern DB. Transcranial amelioration of inflammation and cell death after brain injury. Nature 2014;505:223-228.
12. Tavazzi B, Signoretti S, Lazzarino G, Amorini AM, Delfini R, Cimatti M, *et al.* Cerebral oxidative stress and depression of energy metabolism correlate with severity of diffuse brain injury in rats. Neurosurgery 2005;56:582-589
13. Wefers H, Komai T, Talalay P, Sies H. Protection against reactive oxygen species by nad(p)h: quinone reductase induced by the dietary antioxidant butylated hydroxyanisole (bha). Decreased hepatic low-level chemiluminescence during quinone redox cycling. Febs Lett 1984;169:63-66.
14. Yachie A. Heme oxygenase-1 deficiency and oxidative stress: A review of 9 independent human cases and animal models. Int J Mol Sci 2021;22:1514.
15. Wook CD, Yong CC. Hipk2 modification code for cell death and survival. Mol Cell Oncol 2014;1:e955999.
16. de la Vega L, Grishina I, Moreno R, Kruger M, Braun T, Schmitz ML. A redox-regulated sumo/acetylation switch of hipk2 controls the survival threshold to oxidative stress. Mol Cell 2012;46:472-483.
17. Hofmann TG, Jaffray E, Stollberg N, Hay RT, Will H. Regulation of homeodomain-interacting protein kinase 2 (hipk2) effector function through dynamic small ubiquitin-related modifier-1 (sumo-1) modification. J Biol Chem 2005;280:29224-29232.
18. Saul VV, de la Vega L, Milanovic M, Krüger M, Braun T, Fritz-Wolf K, *et al.* Hipk2 kinase activity depends on cis-autophosphorylation of its activation loop. J Mol Cell Biol

2013;5:27-38.
19. Saul VV, Schmitz ML. Posttranslational modifications regulate hipk2, a driver of proliferative diseases. J Mol Med (Berl). 2013;91:1051-1058.
20. de la Vega L, Grishina I, Moreno R, Krüger M, Braun T, Schmitz ML. A redox-regulated sumo/acetylation switch of hipk2 controls the survival threshold to oxidative stress. Mol Cell 2012;46:472-483.
21. Li R, Shang J, Zhou W, Jiang L, Xie D, Tu G. Overexpression of hipk2 attenuates spinal cord injury in rats by modulating apoptosis, oxidative stress, and inflammation. Biomed Pharmacother 2018;103:127-134.
22. Wiatrak B, Kubis-Kubiak A, Piwowar A, Barg E. Pc12 cell line: cell types, coating of culture vessels, differentiation and other culture conditions. Cells-Basel 2020;9:958.
23. Taylor S, Wakem M, Dijkman G, Alsarraj M, Nguyen M. A practical approach to rt-qpcr-publishing data that conform to the miqe guidelines. Methods 2010;50:S1-S5.
24. Osier N, Dixon CE. The controlled cortical impact model of experimental brain trauma: Overview, research applications, and protocol. Methods Mol Biol 2016;1462:177-192.
25. Loane DJ, Byrnes KR. Role of microglia in neurotrauma. Neurotherapeutics 2010;7:366-377.
26. Hopp S, Nolte MW, Stetter C, Kleinschnitz C, Sirén A, Albert-Weissenberger C. Alleviation of secondary brain injury, posttraumatic inflammation, and brain edema formation by inhibition of factor xiia. J Neuroinflamm 2017;14:39.
27. Verweij BH, Muizelaar JP, Vinas FC, Peterson PL, Xiong Y, Lee CP. Impaired cerebral mitochondrial function after traumatic brain injury in humans. J Neurosurg 2000;93:815-820.
28. Roth TL, Nayak D, Atanasijevic T, Koretsky AP, Latour LL, McGavern DB. Transcranial amelioration of inflammation and cell death after brain injury. Nature 2014;505:223-228.
29. Kahles T, Brandes RP. Nadph oxidases as therapeutic targets in ischemic stroke. Cell Mol Life Sci 2012;69:2345-2363.
30. Ouyang YB, Stary CM, White RE, Giffard RG. The use of microrna to modulate redox and immune response to stroke. Antioxid Redox Signal 2015;22:187-202.
31. Dinkova-Kostova AT, Talalay P. Nad(p)h:Quinone acceptor oxidoreductase 1 (nqo1), a multifunctional antioxidant enzyme and exceptionally versatile cytoprotector. Arch Biochem Biophys 2010;501:116-123.
32. Prochaska HJ, Talalay P, Sies H. Direct protective effect of nad(p)h:Quinone reductase against menadione-induced chemiluminescence of postmitochondrial fractions of mouse liver. J Biol Chem 1987;262:1931-1934.
33. Ross D, Siegel D. The diverse functionality of nqo1 and its roles in redox control. Redox Biol 2021;41:101950.
34. Siegel D, Gustafson DL, Dehn DL, Han JY, Boonchoong P, Berliner LJ, *et al*. Nad(p)h:quinone oxidoreductase 1: role as a superoxide scavenger. Mol Pharmacol 2004;65:1238-1247.
35. Raina AK, Templeton DJ, Deak JC, Perry G, Smith MA. Quinone reductase (nqo1), a sensitive redox indicator, is increased in alzheimer's disease. Redox Rep 1999;4:23-27.
36. Loboda A, Damulewicz M, Pyza E, Jozkowicz A, Dulak J. Role of nrf2/ho-1 system in development, oxidative stress response and diseases: an evolutionarily conserved mechanism. Cell Mol Life Sci 2016;73:3221-3247.
37. Ryter SW. Heme oxgenase-1, a cardinal modulator of regulated cell death and inflammation. Cells-Basel 2021;10:515.
38. Sardina F, Conte A, Paladino S, Pierantoni GM, Rinaldo C. Hipk2 in the physiology of nervous system and its implications in neurological disorders. Biochim Biophys Acta Mol Cell Res 2023;1870:119465.
39. Sung KS, Lee Y, Kim ET, Lee S, Ahn J, Choi CY. Role of the sumo-interacting motif in hipk2 targeting to the pml nuclear bodies and regulation of p53. Exp Cell Res 2011;317:1060-1070.
40. Zou F, Xu J, Fu H, Cao J, Mao H, Gong M, *et al*. Different functions of hipk2 and ctbp2 in traumatic brain injury. J Mol Neurosci 2013;49:395-408.
41. Moehlenbrink J, Bitomsky N, Hofmann TG. Hypoxia suppresses chemotherapeutic drug-induced p53 serine 46 phosphorylation by triggering hipk2 degradation. Cancer Lett 2010;292:119-124.